ORIGINAL PAPER

Diacidic ionic liquid supported on magnetic-silica nanocomposite: a novel, stable, and reusable catalyst for selective diester production

Reza Fareghi-Alamdari[1] · Mehri Nadiri Niri[1] · Hassan Hazarkhani[2] · Negar Zekri[1]

Abstract

Abstract Supported diacidic ionic liquid on magnetic silica nanoparticles (SDAIL@magnetic nanoSiO$_2$) was successfully prepared through a multi-step approach. 2,2- bis ((3- methylimidazolidin-1-yl) methyl) propane- 1,3- diol bromide salt was immobilized onto the surface of magnetic silica nanoparticles via covalent bonding to prepare a novel powerful acidic catalyst. The synthesized catalyst was characterized by FT-IR, SEM, TGA, VSM, N$_2$ adsorption–desorption measurements and acid-base titration. The catalytic activity of the prepared SDAIL@magnetic nanoSiO$_2$ was investigated for the selective diesterification of alcohols by phthalic anhydride to afford corresponding dialkyl plasticizers under solvent-free conditions. The nature of two acidic counter anions as well as the presence of Lewis acidic species (Fe$_3$O$_4$) on the magnetic nanosilica and high surface area of the nanosilica influenced the behavior of the catalyst. Surprisingly, the high acidic character of the catalyst facilitates the reaction with a short reaction time. Furthermore, TG analysis strongly demonstrates that major content of IL is still stable on the support up to 290 °C, so catalyst has a good thermal stability. Under the optimized conditions, the conversion of phthalic anhydride was 100% and diester plasticizers were obtained with excellent yields (80–100%). The SDAIL@magnetic nanoSiO$_2$ catalyst showed a good reusability and could be easily separated from the reaction mixture using an external magnet thanks to its superparamagnetic behavior and reused for several runs without significant activity loss. An important advantage of the SDAIL@magnetic nanoSiO$_2$ was its high-hydrophilicity resulted in excellent selectivity towards the formation of only diesters which are commonly used plasticizers in different industries.
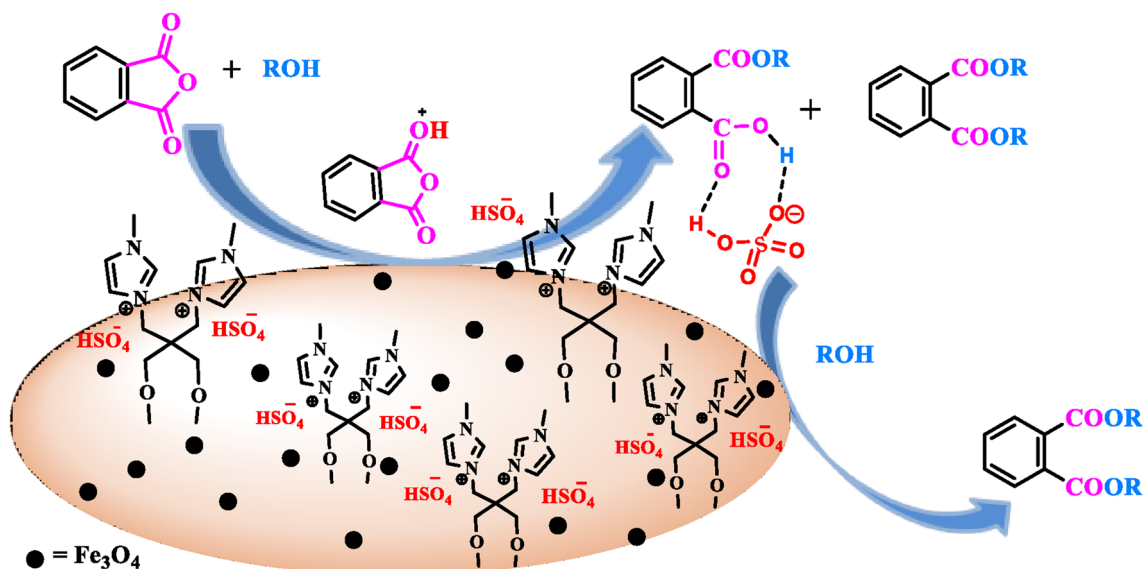
Extended author information available on the last page of the article

Graphical abstract

Introduction

Plasticizers are low molecular weight materials added to polymeric materials, such as paints, plastics or adhesives to improve their original properties [1]. They decrease the glass transition temperature of the polymer and make materials more flexible [2]. One of the most popular groups of plasticizers is ester plasticizers which are a class of the neutral plasticizers. Additionally, the most common ester plasticizers are diesters such as diethyl, dibutyl, and dioctyl phthalates, which are used in formulation of double-based propellants [3]. As shown in Fig. 1, the main function of these compounds is to locate between polymer molecules and increase polymer free volume, consequently, polymer chains easily slip on each other. Therefore, the plasticizers make the polymer soft and pliable by reducing the viscosity and glass transition temperature of polymer [4].

In other words, diesters are important organic compounds which are used as an intermediate in the synthesis
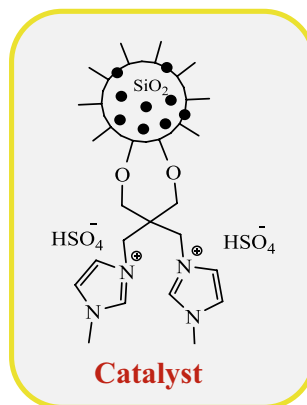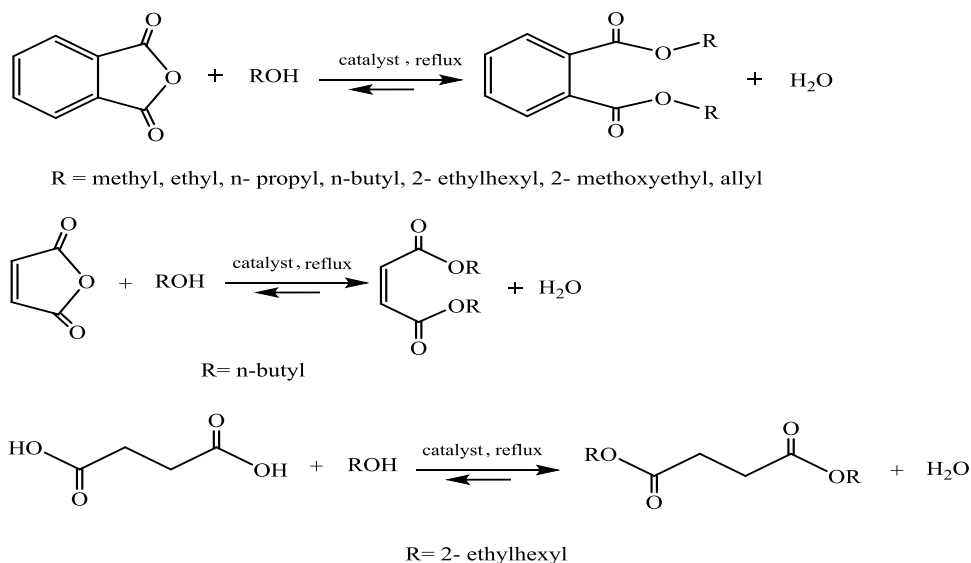
of fine chemicals [5], drugs [6], plasticizers [7, 8], chiral-auxiliaries [9], agrochemicals [10]. Different catalysts have been used to promote the synthesis of diesters [11–13]; most of these protocols need a high loading of expensive and nonrecoverable catalysts and long reaction time in many instances. In addition, the selectivity of the catalyst towards the synthesis of diesters is not always satisfactory.

Selectivity of catalyst is also an important factor in esterification processes of anhydrides or double carboxylic acids with alcohols to synthesize their relative diesters. The selective esterification using mesoporous Si-MCM-41, clay and alumina supported metal Lewis acid, such as $InCl_3$ and $GaCl_3$, as catalyst have been reported [14–16]. However, use of these materials as catalyst, has two main problems. First of all the main product of the esterification reaction is monoester not diester, and the second problem is that these metal species are toxic and/or expensive. Hence, there is still a need to develop a suitable method for the selective diesterification of anhydrides using more efficient catalysts.

Because of the inherent properties of magnetic nanoparticles, such as biocompatibility, easy recovery by magnetic separation, thermal stability against degradation, reaction rates closer to homogeneous counterparts, large surface area, high loading of active sites as well as low toxicity and price, these materials have emerged as a useful group of heterogeneous catalysts [17–22]. These catalysts have been widely applied as magnetically separable catalysts

Fig. 1 Interaction of plasticizer and polymer

Scheme 1 Synthesis of diesters from different alcohols in the presence of SDAIL@magnetic nanoSiO$_2$ catalyst

R = methyl, ethyl, n- propyl, n-butyl, 2- ethylhexyl, 2- methoxyethyl, allyl

R= n-butyl

R= 2- ethylhexyl

Catalyst

in organic reactions [23–32]. However, limited reports are available on ionic liquid supported MNPs as recyclable catalysts for esterification reaction.

With a view of these considerations, and as part of a continuing effort in our laboratory towards the synthesis and application of ionic liquids in the organic synthesis [33–36], and as ionic liquids show high-selectivity in organic reactions [37–40], herein, we wish to disclose a new magnetic highly acidic and reusable catalyst (SDAIL@magnetic nanoSiO$_2$) for diesterification of phthalic and maleic anhydrides as well as succinic acid under solvent-free conditions. On the other hand, a hydrophil and efficient catalytic system with suitable surface properties for the selective production of diesters has been developed in this study (Scheme 1).

We believe that double site for immobilization and at the same time double catalysis site in the structure of our prepared catalyst can improve its efficiency in both terms of stability and activity.

Also the hydrophilic surface of the prepared catalyst indeed provides a means of departure of diester from the catalyst surface as soon as it is produced, thus under appropriate conditions no monoester compound is formed.

Experimental section

Chemicals and instruments

All chemicals and solvents were purchased from Merck and Fluka chemical companies. Melting point was determined using melting point IA 8103 apparatus. ^{1}H NMR and ^{13}C NMR spectra were recorded in DMSO-(d$_6$) and D$_2$O solvents using Brucker-Avance 500 and 125 MHz spectrometer, respectively, and TMS as an internal standard. FT-IR spectroscopy (KBr pellets in the range of 400–4000 cm^{-1} with a Nicolet-860 spectrometer) was employed for characterization of the catalyst and synthesized compounds. The N$_2$ adsorption/desorption isotherms were measured

using a Micrometrics Tristar II 3020 instrument. Thermal gravimetric analysis (TGA) was recorded using a thermal analysis instrument Perkin Elmer (Pyris Diamond model). In this method, runs were carried out in 40 μL alumina pans and under an inert atmosphere of nitrogen at a flow rate of 15 mL min^{-1}. Initial mass introduced in the pan was set at 10 ± 1 mg. Dynamic measurements were conducted at 25–600 °C. The magnetic measurement of sample was carried out in a vibrating sample magnetometer (VSM) (4 in., Daghigh Meghnatis Kashan Co., Kashan, Iran) at room temperature. The scanning electron micrographs (SEM) were obtained on a Philips XL-30 ESEM instrument and transmission electron microscopy (TEM) analysis was recorded on a Philips CM-10 instrument with an accelerating voltage of 100 kV. Elemental analysis for C, H, and N were performed using a Heraeus CHN Rapid analyzer. Quantitative product analysis was conducted by gas chromatography on Hewlett Packard HP-5890 instrument equipped with HP-1 column (30 m long, 0.5 mm diameter), and flame ionization detector (FDI), using N_2 as carrier gas at a flow rate of 2 mL min^{-1}. The reaction monitoring was accomplished by TLC on silica gel PolyGram SILG/UV254 plates. The nanosilica support (Fumed silica S5130 purchased from Sigma chemical company) was dried at 250 °C for 6 h before use. All solvents were strictly dried according to standard operations and stored over 4A° molecular sieves.

Preparation of supported diacidic ionic liquid on magnetic silica nanoparticles (SDAIL@magnetic nanoSiO$_2$)

A multi-step methodology was employed for the synthesis of catalyst in this study as described below:

Preparation of 2,2- bis ((3- methylimidazolidin-1-yl) methyl) propane- 1,3- diol bromide salt (IL-Br)

The IL-Br salt was synthesized according to our previous work [41]. A mixture of 0.52 g 1-methylimidazole (6.25 mmol, 0.5 mL) and 0.65 g 2,2- bis (bromomethyl) -1,3- propanediol (2.5 mmol) was heated at 150 °C for 8 h under magnetic stirring. After cooling to room temperature, the obtained solid was washed three times with acetonitrile and the residue was dried in an oven at 100 °C for 2 h, giving IL-Br as a white powder (yield: 95%, melting point = 150 °C). FT-IR (KBr) ν_{max} = 620.8, 770.7, 829.8, 1060.5, 1164.9, 1450.8, 1573.1, 1760.4, 1655.9, 2935.4, 3260.7 cm^{-1}. ^{1}H NMR (500 MHz, DMSO-d$_6$): δ (ppm) 3.24 (s, 4H, C$\underline{H}_2$N), 3.84 (s, 6H, C$\underline{H}_3$), 4.31 (s, 4H, C$\underline{H}_2$OH), 4.72 (s, 2H, O$\underline{H}$), 7.42 (dd, J = 10 Hz, J = 5 Hz, 4H, C$\underline{H}$=C$\underline{H}$), 8.72 (s, 2H, NC$\underline{H}$N). ^{13}C NMR (125 MHz, DMSO-d$_6$): δ (ppm) 35.94, 45.21, 48.58, 58.48, 123.72, 123.86, 137.38.

Synthesis of Fe$_3$O$_4$ supported silica nanoparticles (magnetic silica nanoparticles)

Magnetite (Fe$_3$O$_4$) nanoparticles were prepared according to the reported method in the literature [42] in a chemical co-precipitation step of ferric and ferrous ions in an alkaline solution. An aqueous solution of FeCl$_3$·4H$_2$O (2.0 g in 10 mL deionized water) was mixed with an aqueous solution of FeCl$_2$·6H$_2$O (0.8 g in 10 mL deionized water). The mixture was stirred vigorously at 80 °C for 30 min, and then this solution was dropped to the 250 mL round bottom flask containing 100 mL of ammonium hydroxide (25% aqueous solution) and the pH value of the solution was adjusted to 9. The reaction was further stirred for another 2 h at 80 °C to afford Fe$_3$O$_4$ nanoparticles as a black precipitate. After completion of the reaction, the black precipitate (Fe$_3$O$_4$) was collected with an external magnet under the reaction flask. The obtained Fe$_3$O$_4$ NPs were washed using deionized water and dried at 80 °C in an oven under vacuum.

To synthesis of Fe$_3$O$_4$ supported silica nanoparticles (Fe$_3$O$_4$ @ SiO$_2$), silica nanoparticles were dried in an oven at 250 °C for 6 h before using. 0.8 g of dried silica nanoparticles were dispersed in dry methanol (10 mL), then 0.2 g of Fe$_3$O$_4$ NPs were added to this solution. The resultant mixture was allowed to stirr at room temperature for 24 h, then the solvent was evaporated with rotary under reduced pressure to give Fe$_3$O$_4$ @ SiO$_2$. Finally, the obtained material was dried at 80 °C under vacuum.

Preparation of magnetic nanosilica chloride

The methodology used to obtain magnetic nanosilica chloride was previously reported in the literature [43]. Magnetic silica nanoparticles (0.4 g) were placed in an oven at 200 °C for 1 h to dry it. Thionyl chloride (5 mL) was then dropped slowly over 15 min and the reaction continued at room temperature for 1 h with stirring. Then the mixture was refluxed for about 3 h at 70 °C in an oil bath. The resulting compound was placed in a vacuum desiccator for 24 h to obtain the yellow powder of magnetic nanosilica chloride.

Preparation of Fe$_3$O$_4$ @ SiO$_2$-IL-Br

2,2- bis ((3- methylimidazolidin-1-yl) methyl) propane- 1,3- diol bromide salt (IL-Br) (2 mmol, 0.85 g) was added to the round bottom flask containing magnetic nanosilica chloride (0.5 g) and NaH (4 mmol, 0.01 g) in 25 mL of dry toluene and the mixture was refluxed for 24 h with stirring. The resulting solid was filtered out, washed twice with dry toluene and dried at 80 °C for 5 h in an oven under vacuum to give Fe$_3$O$_4$ @ SiO$_2$-IL-Br.

Preparation of SDAIL@magnetic nanoSiO$_2$

The SDAIL@magnetic nanoSiO$_2$ was synthesized by anion exchange of Fe$_3$O$_4$ @ SiO$_2$-IL-Br. 0.74 g of Fe$_3$O$_4$ @ SiO$_2$-IL-Br was dispersed in methanol (30 mL) under stirring. Then 0.23 mL sulfuric acid (4 mmol) was dropped slowly and the mixture was refluxed for 24 h at 60 °C. After completion of the reaction, the solvent was evaporated under vacuum. The resulting material was washed with dichloromethane (3×5 mL) and dried in an oven at 150 °C for 2 h to afford SDAIL@magnetic nanoSiO$_2$ as a brown powder.

General procedure for diesterification of alcohols by SDAIL@magnetic nanoSiO$_2$

Weighed amounts of anhydrides or acid, alcohol and catalyst, were added to round bottom flask with a dean–stark apparatus, reflux condenser and a magnetic stirrer. The esterification reaction was typically carried out for 2–10 h at the desired temperature with vigorous stirring. The catalyst could be easily recovered from the reaction mixture using an external magnet due to its magnetic property without any disposal. Then the product was separated simply by decantation with ethyl acetate. Ethyl acetate was removed under reduced pressure to afford pure desired product.

Typical procedure for diesterification of 2-methoxyethanol by SDAIL@magnetic nanoSiO$_2$ as catalyst

The required amounts of phthalic anhydride (1 mmol, 0.15 g), 2- methoxyethanol (5 mmol, 0.39 mL, 0.38 g) and SDAIL@magnetic nanoSiO$_2$ as catalyst (10 wt% to phthalic anhydride, 0.01 g) were added successively into a 50 mL round bottom flask with a dean–stark apparatus, reflux condenser and a magnetic stirrer. The esterification reaction was allowed to proceed at 130 °C for.8 h under vigorous stirring. The completion of reaction was monitored by TLC using (EtOAC/Hexane 2:8) as eluent. After completion of the reaction, the catalyst was recovered from the reaction mixture using an external magnet and subjected to drying under high vacuum at 70 ∘C for 6 h to remove water, leaving behind the SDAIL@magnetic nanoSiO$_2$ (recovery 98%) which was recycled. Then, the product (bis (2- methoxyethyl) phthalate) was separated simply by extraction with ethyl acetate (3×5 mL) and ethyl acetate was evaporated under vacuum to afford desired product as colorless oily liquid at 98% yield (0/25 g, boiling point = 340 °C). The obtained product dried under vacuum at 70 °C for 6 h.

Spectral and analytical data of some products

bis (2- methoxyethyl) phthalate

FT-IR (KBr) ν_{max} = 745, 1281, 1448, 1600, 1726, 2884, 3080 cm^{-1}. ^{1}HNMR (100 MHz, CDCl$_3$): δ (ppm) 3.41 (s, 6H, C$\underline{H}_3$–O), 3.70 (t, J = 1 Hz, 4H, O-C$\underline{H}_2$-CH$_2$-O), 4.47 (t, J = 2 Hz, 4H, O-CH$_2$-C$\underline{H}_2$-O), 7.54 (d, J = 2 Hz, 2H, C$\underline{H}$ = CH), 7.75 (d, J = 1 Hz, 2H, CH = C$\underline{H}$). Anal. Cald. for C$_{14}$H$_{18}$O$_6$ (282.29): C, 59.51; H, 6.38. Found: C, 59.53; H, 6.42.

Diallyl phthalate

FT-IR (KBr) ν_{max} = 745, 1123, 1271, 1449, 1601, 1728, 2926, 3083 cm^{-1}. ^{1}HNMR (100 MHz, CDCl$_3$): δ (ppm) 4.83 (d, J = 1 Hz, 4H, C$\underline{H}_2$-CH = CH$_2$), 5.33 (d, J = 7 Hz, 2H, CH$_2$-CH = C$\underline{H}_2$), 5.45 (d, J = 4 Hz, 2H, CH$_2$-CH = C$\underline{H}_2$), 6.05 (m, 2H, CH$_2$-C$\underline{H}$ = CH$_2$), 7.59 (d, J = 5 Hz, 2H, C$\underline{H}$ = CH), 7.79 (m, 2H, CH = C$\underline{H}$). Anal. Cald. for C$_{14}$H$_{14}$O$_4$ (246.26): C, 68.22; H, 5.69. Found: C, 68.25; H, 5.71.

Dipropyl phthalate

FT-IR (KBr) ν_{max} = 743, 1124, 1275, 1464, 1721, 2968, 3071 cm^{-1}. ^{1}HNMR (100 MHz, CDCl$_3$): δ (ppm) 1.13 (t, J = 2 Hz, 6H, CH$_3$-), 1.94 (m, 4H, CH$_3$-C$\underline{H}_2$-CH$_2$), 4.07 (t, J = 2 Hz, 4H, CH$_3$-CH$_2$-C$\underline{H}_2$-O), 7.70 (d, J = 2 Hz, 2H, CH = CH). Anal. Cald. for C$_{14}$H$_{18}$O$_4$ (250.29): C, 67.12; H, 7.19. Found: C, 67.16; H, 7.22.

Results and discussion

Immobilization of ionic liquid onto the surface of magnetic support via covalent bonding

The ionic liquid can be bounded or supported on a solid support surface via two distinct approaches. The first approach involves the simple adsorption of the ionic liquid onto the surface of the solid support (physical bonding) whereas the second approach involves the covalent attachment of ionic liquid to the solid support surface (chemical bonding). The former has a serious drawback of leaching of ionic liquid during vigorous reaction conditions. Thus, the chemical bonding has more advantageous for catalytic applications.

In this approach, the ionic liquid could be covalently bonded to the solid support surface via the cation or anion. SDAIL@magnetic nanoSiO$_2$ as catalyst was prepared based on the following procedure (Scheme 2). At first, the precursor ionic liquid was prepared by nucleophilic substitution reaction of 1- methylimidazole and 2,2- bis (bromomethyl)-1,3- propanediol. Then magnetic nanosilica chloride easily synthesized via nucleophilic substitution reaction between

Scheme 2 Multi- step route for the synthesis of SDAIL@ magnetic nanoSiO$_2$
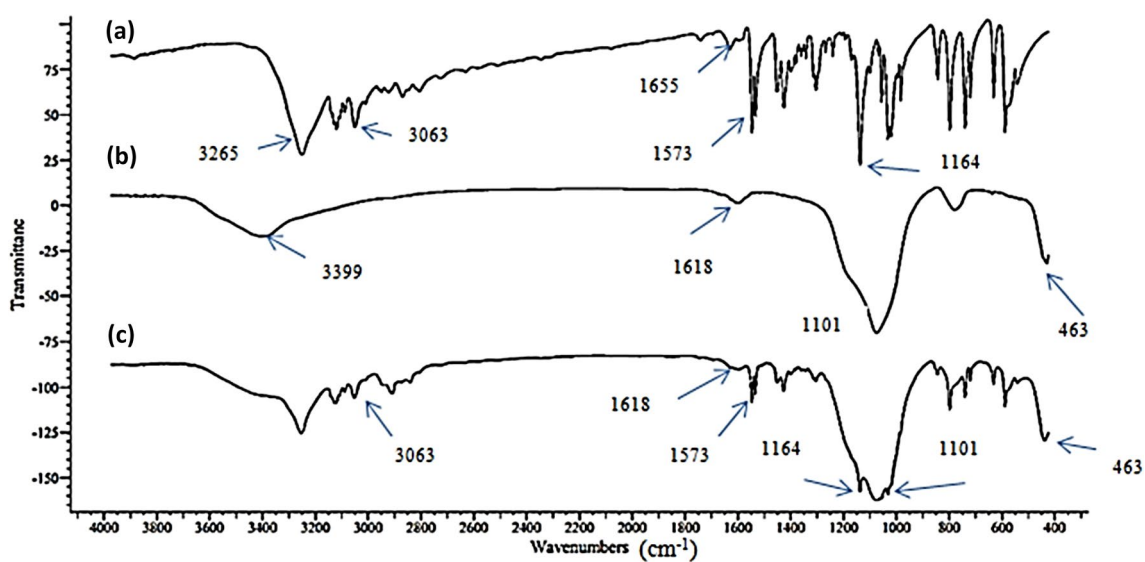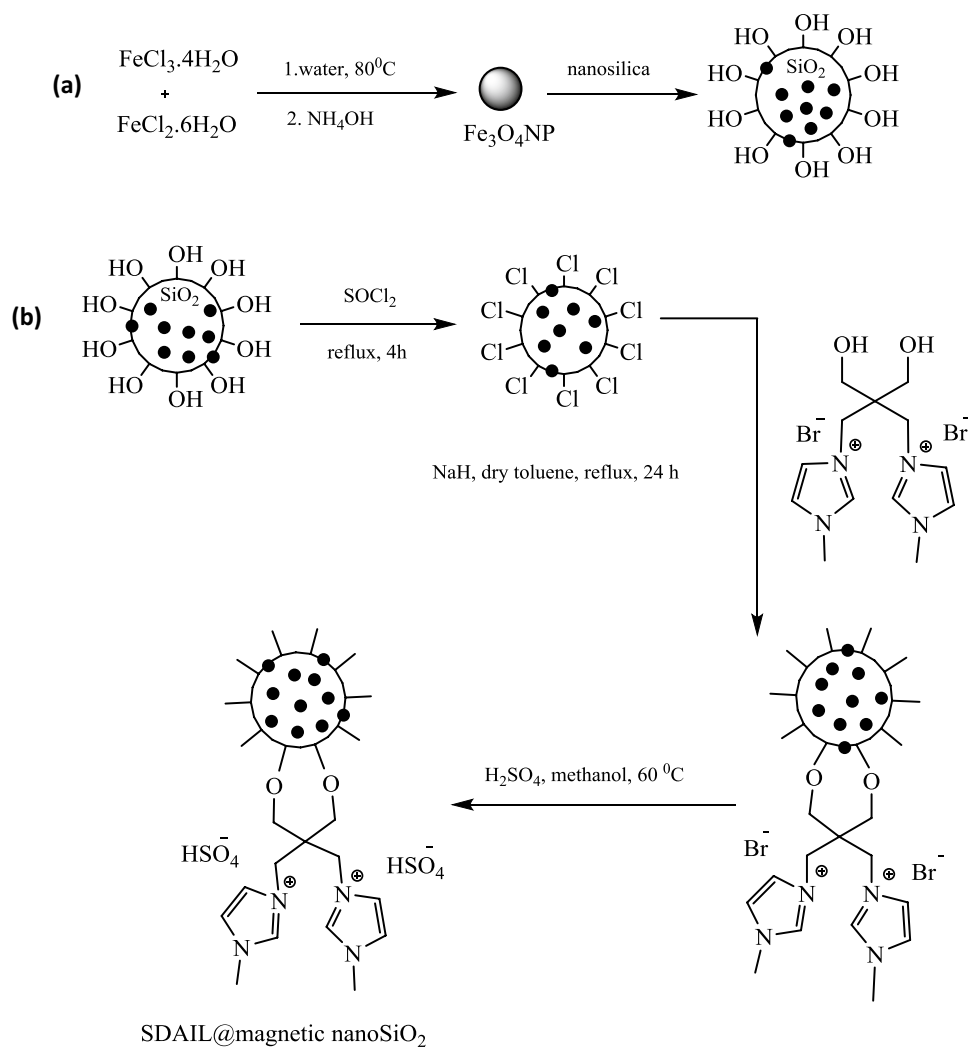
Fig. 2 FT-IR spectra of (a) pure ionic liquid, (b) magnetic nanosilica chloride, and (c) SDAIL@magnetic nanoSiO$_2$

magnetic silica nanoparticles and thionyl chloride. After the grafting of the ionic liquid to the magnetic nanosilica chloride through covalent bonds, the obtained compound converted to the SDAIL@magnetic nanoSiO$_2$ by an anion exchange step with sulfuric acid. The catalytic activity of this catalyst was investigated in the synthesis of diesters.

Characterization of SDAIL@magnetic nanoSiO$_2$ catalyst

The prepared magnetic catalyst was characterized using different techniques such as scanning electron microscopy (SEM), transmission electron microscopy (TEM), FT-IR, N$_2$ adsorption/desorption measurement, thermal gravimetric analysis, and vibrating sample magnetometer.

The amount of H$^+$ in the catalyst, which was determined by acid–base titration against a standard NaOH solution with phenolphthalein as indicator, was obtained 6.16 mmol/g.

FT-IR was employed to witness the successful functionalization of magnetic nanosilica chloride with acidic ionic liquid and to characterize organic functionalities. Figure 2 presents the FT-IR spectra of pure ionic liquid (a), magnetic nanosilica chloride (b) and SDAIL@magnetic nanoSiO$_2$ (c). As shown in Fig. 2a, the characteristic bonds of pure ionic liquid (IL-Br) around 3265, 3063, 2935, 1655 and 1065 cm^{-1} attribute to the O–H, =C–H, –C–H, C=N and C–N stretching vibrations. The peaks at 1450 and 1573 cm^{-1} correspond to the C=C stretching vibrations of the imidazole ring and the strong bond at 1164 cm^{-1} assigns to the C–O stretching vibration also. For magnetic nanosilica chloride (Fig. 2b), the bonds at 463 and 1618 cm^{-1} represent the stretching vibrations of the Fe–O bond in Fe$_3$O$_4$ [44]. The strong band at 1101 cm^{-1} belongs to the Si–O stretching vibration and the broad peak at 3399 cm^{-1} corresponds to the stretching vibration of Si–OH group. In the FT-IR spectra of SDAIL@magnetic nanoSiO$_2$ (Fig. 2c), apart from the original peaks of magnetic nanosilica chloride, additional peaks attributed to the functional groups of the IL-Br also
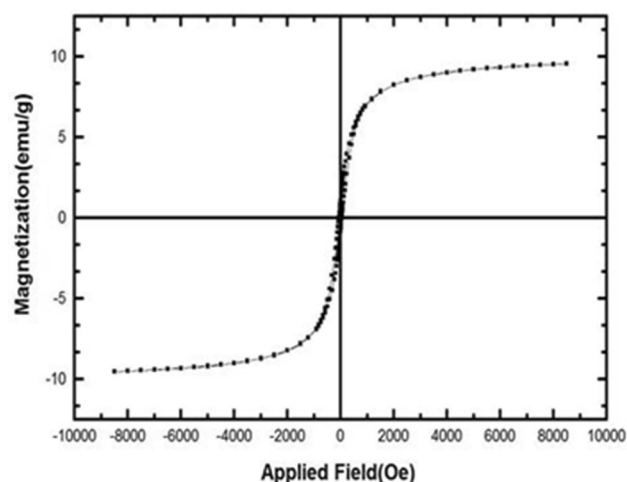

Fig. 4 Magnetization curve of SDAIL@magnetic nanoSiO$_2$

observed, but the intensity of the peaks decreased notably. Therefore, the above results prove that the IL-Br ionic liquid was successfully bonded with magnetic nanosilica chloride.

The surface morphology and nanocomposite nature of SDAIL@magnetic nanoSiO$_2$ were characterized by the scanning electron microscopy (SEM) and transmission electron microscopy (TEM) techniques, respectively. SEM images for typical nanosilica samples before and after IL supporting are shown in Fig. 3a, b. The SEM images reveal that nanosilica support contains nanoparticles with the average size of 40 nm (Fig. 3a). As shown in Fig. 3b, SDAIL@magnetic nanoSiO$_2$ catalyst has uniform and spherical morphology and the average size of the obtained particles is 48 nm. Comparing the images of Fig. 3a, b shows that the morphological homogeneity is maintained after supporting of IL and no obvious aggregation of the silica nanoparticles was detected after immobilization of IL which demonstrates that the particles of nanosilica have a good mechanical stability during the supporting process.
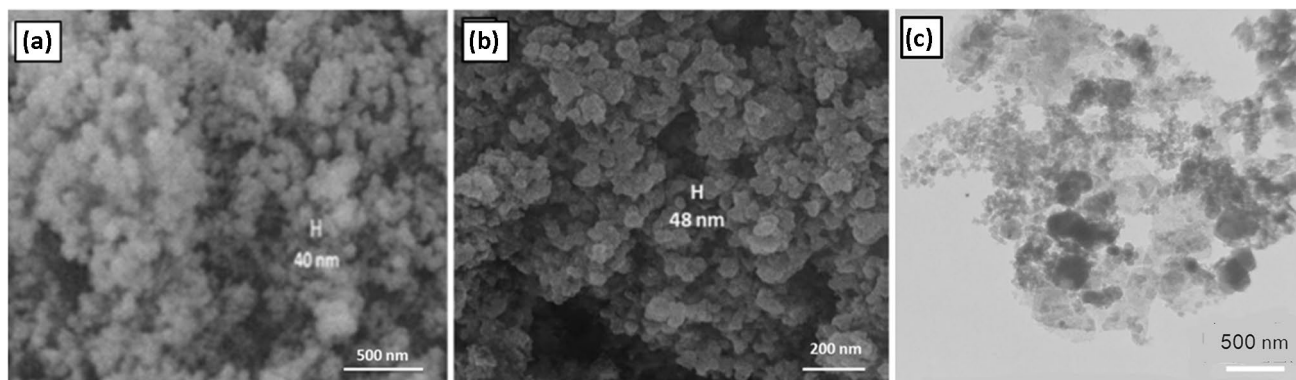

Fig. 3 SEM images of **a** nanosilica **b** SDAIL@magnetic nanoSiO$_2$ and **c** TEM image of SDAIL@magnetic nanoSiO$_2$

TEM observations clearly reveal the nanocomposite structure of the SDAIL@magnetic nanoSiO$_2$ catalyst (Fig. 3c). On the other hand, black iron particles (Fe$_3$O$_4$) were distributed sporadically on spherical nanosized silica particles.

Magnetic measurement for SDAIL@magnetic nanoSiO$_2$ was performed by vibrating sample magnetometer (VSM) technique. Its hysteresis curve is presented in Fig. 4. It can be seen from the curve that the saturation magnetization of SDAIL@magnetic nanoSiO$_2$ is 9.8 emu/g. The high magnetic property of this catalyst is very beneficial in heterogeneous catalysis as it is easily recoverable by external magnetic field.

The thermal stability of SDAIL@magnetic nanoSiO$_2$ was determined by TG analysis through heating from room temperature to 600 °C under nitrogen flow (Fig. 5). Three steps of weight loss are exhibited in the thermogram of catalyst. The TGA curve indicates an initial weight loss of about 18% at the temperature range of 25–210 °C, which is due to the desorption of hydrogen bonded water molecule both on the surface and in the pores of the particles. This high-absorbed water demonstrated that the catalyst surface has hydrophilic character to some extent. This property may make it suitable when its surface is exposed to the hydrophilic reactants. The second weight loss of approximately 41% at 210–348 °C, weight loss of almost 13% at 348–465 °C and in the final step, the weight loss of about 4% appeared at the range of 465–595 °C can be ascribed to decomposition of covalently bonded ionic liquid from the surface of the magnetic nanosilica. So, the amount of organic moiety is about 57% against the total solid catalyst. Additionally, the TGA curve shows that the maximum weight loss of the ionic liquid occurs at 290 °C. Therefore, major content of IL is still stable on the support up to 290 °C and the adhesion of iron particles and ionic liquid on the surface of the nanosilica has been done well.

The corresponding textural parameters such as surface area and pore diameter were determined by Brunauer-Emmet-Teller (BET) technique (Fig. 6; Table 1). The results obtained from N$_2$ adsorption–desorption experiments of pure nanosilica and SDAIL@magnetic nanoSiO$_2$ showed that both samples pure nanosilica and SDAIL@magnetic nanoSiO$_2$ possess type-IV isotherms with H$_3$ hysteresis loop centered at relative pressure of about 0.4–0.8 confirming the mesoporous structure of the materials (Fig. 6a, b). Moreover, the BJH calculation of the SDAIL@magnetic nanoSiO$_2$ (Table 1, entry 2) shows, the pore diameter was decreased after supporting of the ionic liquid on the surface of nanosilica. Additionally, the BJH diagrams of the samples confirm the mesoporous and regular structure of the materials (Fig. 6c, d).

BET surface area measurements indicated that, compared with nanosilica (Table 1, entry 1) the surface area of the SDAIL@magnetic nanoSiO$_2$ (Table 1, entry 2, Fig. 6e, f) was significantly decreased from 399 to 48 m^2 g^{-1}. Presumably, the loading of ionic liquid on the surface of the nanosilica led to this obvious decrease. In other words, the reduction of the surface area verified that the immobilization
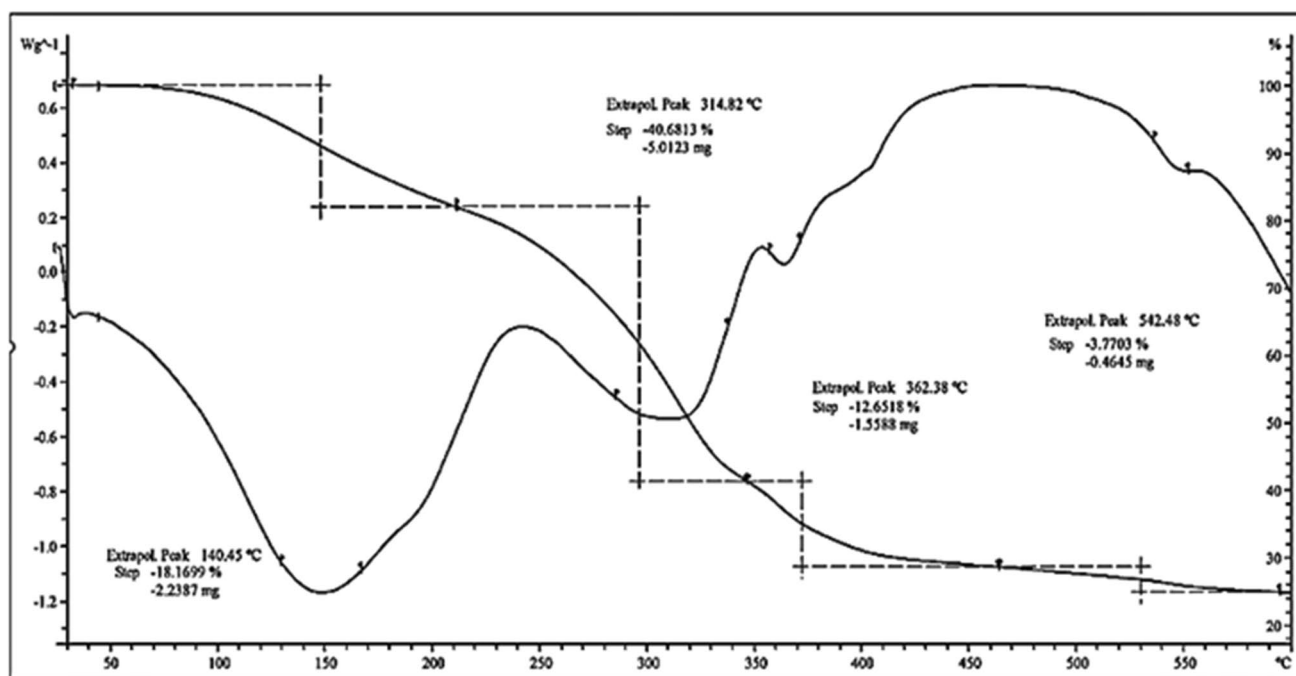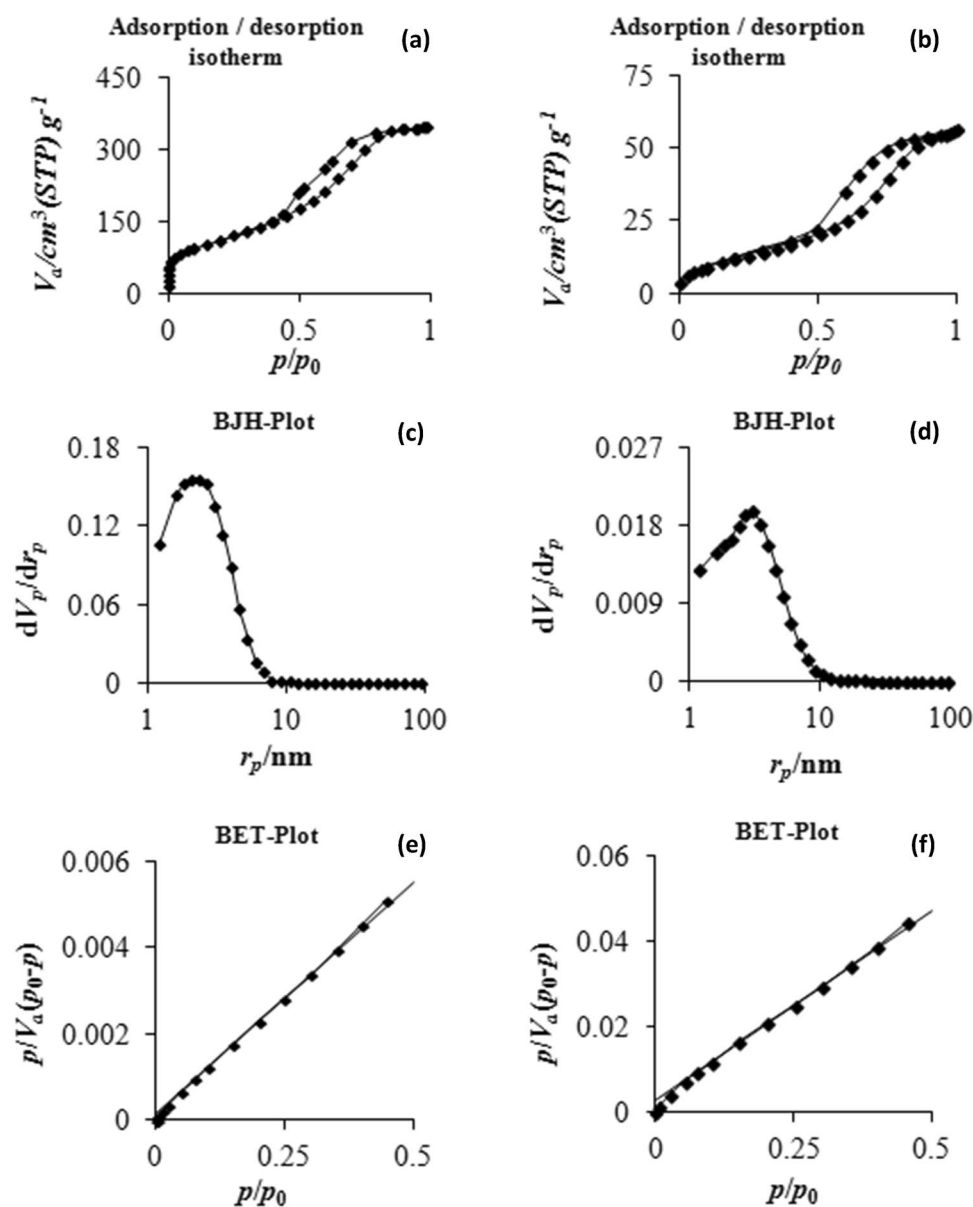

Fig. 5 The TGA curve of SDAIL@magnetic nanoSiO$_2$

Fig. 6 N$_2$ adsorption/desorption isotherms of **a** pure nano-silica and **b** SDAIL@magnetic nanoSiO$_2$, BJH plots of **c** pure nanosilica and **d** SDAIL@magnetic nanoSiO$_2$, BET plots of **e** pure nanosilica and **f** SDAIL@magnetic nanoSiO$_2$

Table 1 Textural parameters of nanosilica and SDAIL@magnetic nanoSiO$_2$

Entry	Sample	BET surface area[a]	BJH desorption average pore width[b]
1	Nanosilica	399	20
2	SDAIL@magnetic nanoSiO$_2$	48	17

[a]BET surface area (m^2 g^{-1})

[b]Average pore width (nm)

of ionic liquid onto the surface of the nanosilica has been successful.

Optimization of esterification reaction conditions

To optimize esterification reaction conditions, we examined the effects of reaction temperature, amount of the catalyst and molar ratio of phthalic anhydride to alcohol in the esterification reaction of phthalic anhydride with butanol in the presence of SDAIL@magnetic nanoSiO$_2$ without any solvent. The results are summarized in

Table 2. As can be seen in this Table, excellent yields of diester products were afforded by SDAIL@magnetic nanoSiO2 catalyst but the best result was obtained under optimized reaction conditions for this esterification reaction which are 10 wt% of catalyst to phthalic anhydride, molar ratio of reactants 1:5 and 125 °C for 2 h. The following is a detailed description of optimized conditions.

In examining the effect of temperature, yield of the reaction was low at 25 °C (Table 2, entry 1). The yield of products were enhanced by increasing the reaction temperature and at temperatures less than 100 °C water evaporation rates are low, so the equilibrium reactions return toward the reactants. It seems that by reaching the reaction temperatures to the boiling point of water, the yield of products improved (Table 2, entries 2–4). It was observed that at higher temperatures, alcohol was quickly evaporated and hence by rising temperature above 125 °C the reaction yield decreased (Table 2, entry 6). So, the optimum reaction temperature for this synthesis process was 125 °C (Table 2, entry 5).

A suitable way to enhance the rate of esterification reaction is increasing the amount of alcohol which promotes the reaction equilibrium toward the product. As shown in Table 2, the reaction yield is enhanced by increasing the molar ratio of butanol to phthalic anhydride and the optimum molar ratio of phthalic anhydride to butanol is suggested to be 1:5 (Table 2, entries 5, 9, 10).

To investigate the optimum amount of SDAIL@magnetic nanoSiO2, different quantities of the catalyst were examined. The yield of products was improved with increasing the catalyst loading (Table 2, entries 5,7). The best result was obtained in the presence of 10 wt% of catalyst (Table 2, entry 5). Higher molar ratios of the catalyst will not improve the yield of reaction (Table 2, entry 8).

Table 2 Optimization of reaction conditions for the esterification reaction of phthalic anhydride with butanol in the presence of SDAIL@magnetic nanoSiO2 as catalyst

Entry	Catalyst (wt %)	Molar ratio of reactants[a]	Temperature (°C)	Time (h)	Yield[a,b] (%)
1	10	1:5	25	24	10
2	10	1:5	50	10	60
3	10	1:5	75	9	95
4	10	1:5	100	5	100
5	10	1:5	125	2	100
6	10	1:5	150	2	80
7	5	1:5	125	5	97
8	15	1:5	125	4	97
9	10	1:2	125	7	80
10	10	1:3.5	125	7	97

Reaction coditions: reactions were carried out under solvent-free conditions

[a]Conversion of phthalic anhydride was 100% in all cases (except for the entries 1 and 2)

[b]Yields refer to the diester products

under solvent-free conditions were obtained. As shown in this Table, values of turn over number (TON) and turn over frequency (TOF) were calculated in the presence of SDAIL@magnetic nanoSiO2 for different diesters. According to Table 3 (entries 1–5) esterification of long alkyl chain alcohols was very satisfactory due to their high-boiling points and lower-boiling point alcohols have lower amounts of TON and TOF. Allyl alcohol and 2- methoxy ethanol led to excellent yields too (entries 6, 7). As shown in Table 3, the highest values of TON and TOF were obtained for bis (2-ethylhexyl) succinate (entry 8). Due to the resonance of the double bond with the carbonyl group in phthalic and
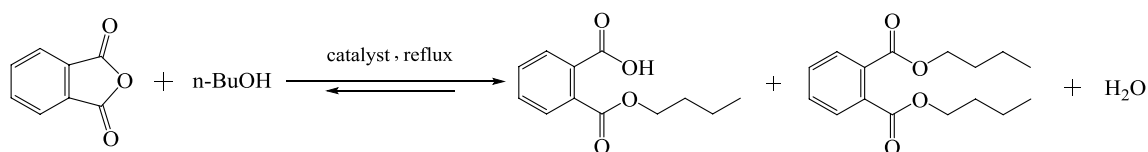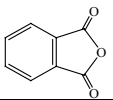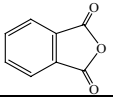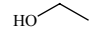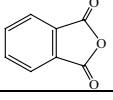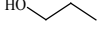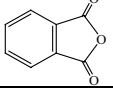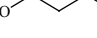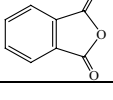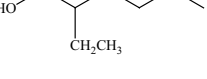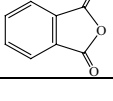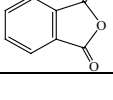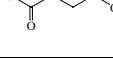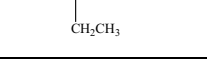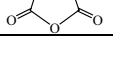

Catalytic activity of SDAIL@magnetic nanoSiO2 for esterification reaction

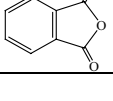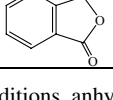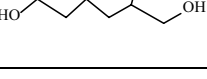The catalytic potential of SDAIL@magnetic nanoSiO2 was investigated for the synthesis of diester plasticizers via the esterification reaction (Table 3). It is clear that SDAIL@ magnetic nanoSiO2 has very high-catalytic activity for esterification reactions and excellent yields ranging from 80 to 100% with perfect conversion of phthalic or maleic anhydride and succinic acid (100%) in short reaction times

maleic anhydride, the electron density is displaced toward carbonyl carbon, while succinic acid does not have such a conjugated double bond. Therefore, carbonyl carbon has a higher positive charge and had better result in esterification reaction (Table 3, entries 8, 9). The above results show that SDAIL@magnetic nanoSiO2 has excellent selectivity for diester products.

Then, we investigated the ability of the catalyst for esterification of butanol and 1, 2, 6-hexanetriol with phthalic anhydride. No product was obtained in these reactions

Table 3 Synthesis of diester plasticizers in the presence of SDAIL@magnetic nanoSiO$_2$ as catalyst

Entry	Anhydride or acid	Alcohol	Temperature °(C)	Time (h)	Yield[a] (%)	TON[b]/TOF[c] (h^{-1})	Measured b.p. (°C)/L b.p. (°C) [Refs.]
1		CH$_3$OH	65	10	80	15.5/1.6	285/284 [45]
2		HO⌒	78	8	95	21.1/2.6	296/295 [45]
3		HO⌒⌒	98	7	95	23.8/3.4	321/Not reported
4		HO⌒⌒⌒	118	2	100	25.8/12.9	340/339-340 [45]
5		HO⌒⌒⌒ CH$_2$CH$_3$	180	1	100	27.9/27.9	387/385 [45]
6		HO⌒⌒	97	5	95	23.4/4.7	293 (New compound)
7		HO⌒⌒O⌒	125	8	98	27.6/3.5	330 (New compound)
8		HO⌒⌒⌒ CH$_2$CH$_3$	180	0.5	100	28.5/57	360/Not reported
9		HO⌒⌒⌒	118	3	100	23.24/7.9	282/Not reported
10		HO⌒⌒⌒OH	235	5	–	–	–
11		HO⌒⌒⌒OH, OH	178	5	–	–	–
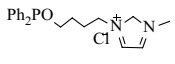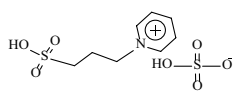
Reaction coditions, anhydrides or acid: alcohol = 1:5, catalyst was 10 wt% to anhydrides or acid

[a]Yields refer to the diester products (GC yield)

[b]*TON* Turn over number, the amount of diester formed (g)\the amount of the catalyst (g)

[c]*TOF* Turn over frequency, the amount of diester formed (g)\(the amount of the catalyst (g) × time (h))

Table 4 Comparison of the efficiency of the catalyst at this work with other reported catalysts in the diesterification reactions

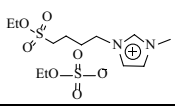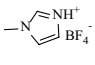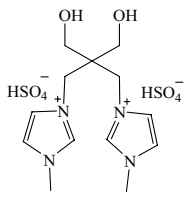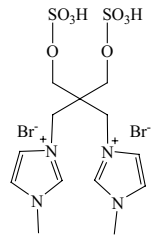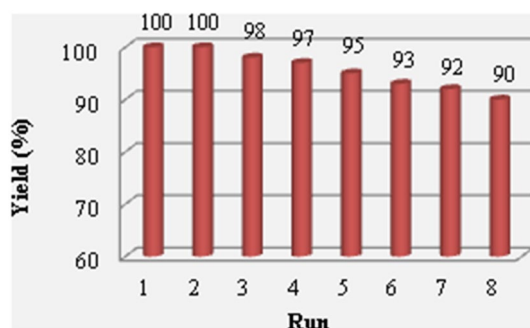| Entry	Catalyst	Acid or anhydride	Alcohol	Amount of catalyst	Acid:alcohol	T (°C)	Time (h)	PhA conv. (%)	Yield[a] (%)	Ref.
1		Phthalic anhydride	Butanol	Excess	1:2	100	3.5	Not reported	78	[46]
2		Phthalic anhydride	2-Ethyl-1-hexanol	15 mol%	1:2.5	115–125	1.5	95	Not reported	[8]
3		Succinic acid	Methanol	20 mol%	1:2	80	4	Not reported	70	[47]
4[b]		Oxalic acid	1-Octanol	2 mL	1:2	110	4	> 99	Not reported	[48]
5[c]	$H_6P_2W_{18}O_{62}$	Phthalic anhydride	Butanol	0.058 mol%	1:2	110	3	91	Not reported	[49]
6[d]	Amorphous zirconium titanium phosphate	Phthalic anhydride	Butanol	0.2 g	1:2.5	115	10	Not reported	62.4	[50]
7	(HFDAIL)	Phthalic anhydride	Butanol	10 mol%	1:5	125	7	100	95	[41]
8	(SFDAIL)	Phthalic anhydride	Butanol	10 mol%	1:5	125	8	100	70	[41]
9	SDAIL@magnetic nanoSiO$_2$	Phthalic anhydride	Butanol	10 wt%	1:5	125	2	100	100	[This work]

[a]Yields refer to the diester products

[b]n (Oxalic acid) = 0.02 mol

[c]The dosage of the catalyst was mol percentage based on phthalic anhydride and mol of phthalic anhydride was 0.3

[d]n (Phthalic anhydride) = 0.025 mol

(Table 3, entries 10 and 11). It seems that a polymer produced instead of the cyclic diester.
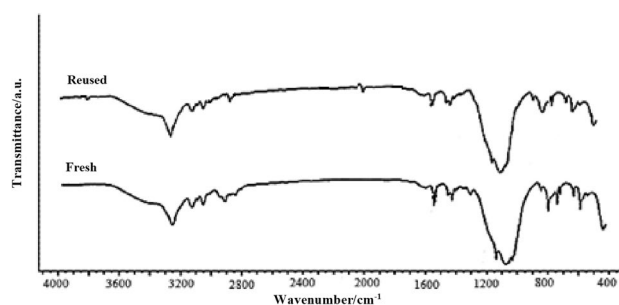
Comparison of the efficiency of SDAIL@ magnetic nanoSiO$_2$ with other reported catalysts in the esterification reaction

A comparative study on the catalytic performance of SDAIL@magnetic nanoSiO$_2$ with the other reported catalysts in the literature as well as the other synthesized catalysts in our previous work for the synthesis of diesters is shown in Table 4. As can be seen in this Table, the catalytic activity of SDAIL@magnetic nanoSiO$_2$ is much better than the other catalysts. The highest yield of diester without contamination by monoester compound was obtained in the presence of the catalyst at this work. It is noteworthy that this result was obtained in the shortest reaction time and with an appropriate amount of the catalyst compared to other catalytic systems.

The high polar nature of ionic liquid containing two HSO$^-_4$ acidic sites and high surface area of the magnetic nanosilica possessing Lewis acidic species (Fe$_3$O$_4$), cooperate with each other to increase the efficiency of the catalyst. Moreover, the high-hydrophilicity of the catalyst, arised from the presence of HSO$^-_4$ anions on it, as well as higher hydrophobicity of diester product compared with monoester one, cause the diester expell from the surface of the catalyst, but the monoester remains on the surface of the catalyst to convert to diester compound. So, excellent selectivity for diester product was observed in the presence of SDAIL@magnetic nanoSiO$_2$. It is noteworthy that the synthesized ionic liquids in our previous work showed excellent results in the synthesis of diesters. However, in the present work, grafting of ionic liquid on the solid support reduced the reaction time and increased selectivity for diester. As a result, the catalytic activity of the catalyst in this work is much better than the other catalytic systems for the esterification reaction.
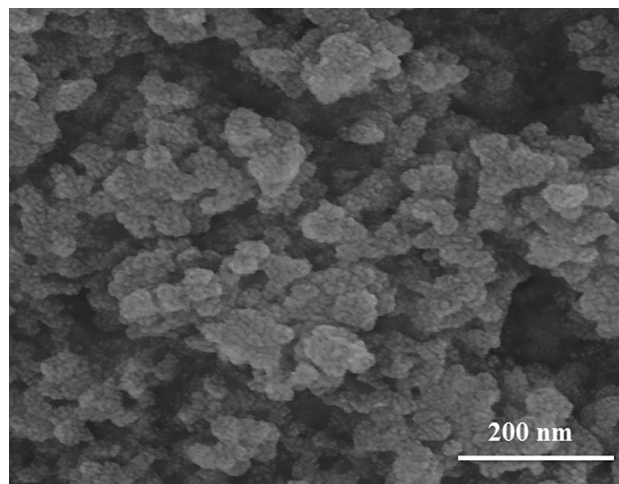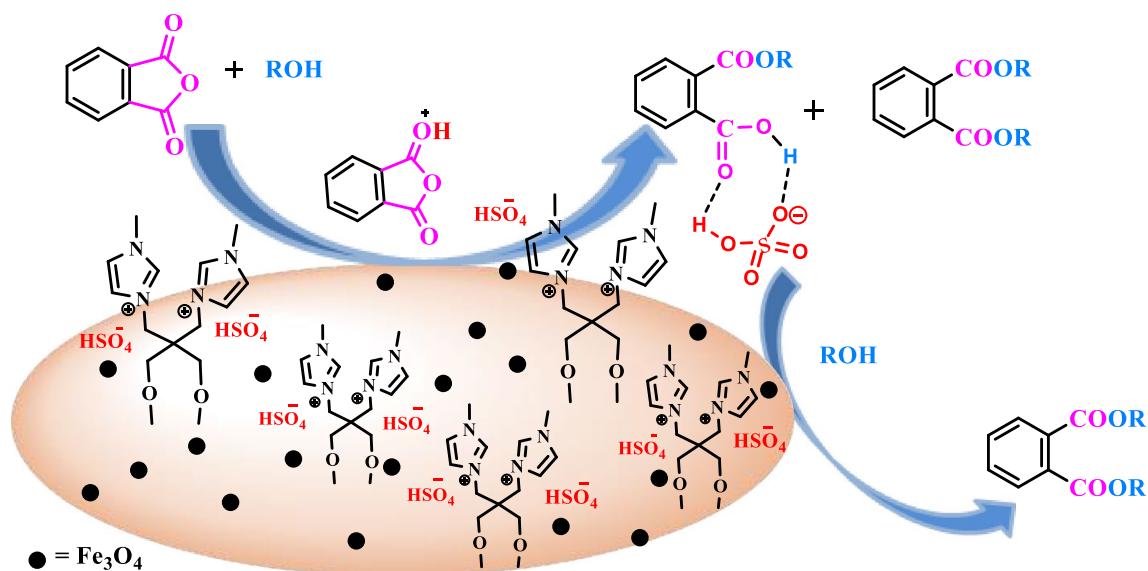

Fig. 8 FT-IR spectrum for the comparison of the fresh catalyst and the eight times reused catalyst

Reusability of SDAIL@magnetic nanoSiO$_2$ in esterification of phthalic anhydride with butanol

The reusability of the SDAIL@magnetic nanoSiO$_2$ catalyst was also studied in the diesterification of phthalic anhydride and butanol as a model reaction. The catalyst was recovered from the reaction mixture by an external magnet, washed with dichloromethane and reused for the next runs with consistent activity even after eight catalytic cycles (Fig. 7). The successful recovery of the catalyst from such reaction accomplishing under harsh condition, highlights the notion that the developed immobilization approach in this study not only provides high-catalytic activity of supported acidic groups, but it also ensure the stability and recoverability of the catalyst under the described reaction conditions. This might be attributed to the anchoring of acidic ionic liquid to the surface via two hydroxyl group.

Fig. 7 Reusability of SDAIL@magnetic nanoSiO$_2$ for diesterification of phthalic anhydride with butanol at optimized reaction condition

Fig. 9 SEM image of eight times reused SDAIL@magnetic nanoSiO$_2$ catalyst

Scheme 3 The proposed reaction mechanism of the synthesis of diesters from phthalic anhydride in the presence of SDAIL@magnetic nanoSiO$_2$
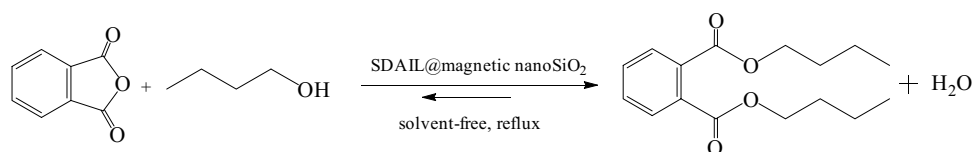
The recovered catalyst after eight runs had no obvious change in structure, referring to the FT-IR spectrum in comparison with the fresh one (Fig. 8). In other words, this figure shows the presence of the ionic liquid in the catalyst after eight runs.

A SEM observation of the recovered catalyst was also made (Fig. 9). By comparing Fig. 3b with Fig. 9, it is evident that there was no obvious change in the morphology of the reused catalyst after eight runs.

Moreover, the stability of the reused SDAIL@magnetic nanoSiO$_2$ was examined by acid–base titration after eight runs. Only a slight loading amount loss of ionic liquid was observed after eight runs. The loading amount of ionic liquid in the nanocatalyst was obtained 5.99 mmol/g. We can conclude that no remarkable leaching of the ionic liquid from the surface of the nanosilica was occured.

The results of the SEM technique, FT-IR spectra and acid–base titration revealed that the catalyst is stable under these reaction conditions.

Reaction mechanism

The suggested reaction mechanism of phthalic anhydride with alcohol in the presence of SDAIL@magnetic nanoSiO$_2$ as an acidic catalyst is shown in Scheme 3. As it shown,

first, the carbonyl group is activated by adsorption of H$^+$ from the catalyst. In the next step, by nucleophilic attack of alcohol on the activated carbonyl group, monoester product is synthesized. The obtained product (monoester) was then subjected to esterification reaction by the addition of second mole of alcohol. Due to the hydrophilicity of catalyst and hydrophobicity of diester than monoester, the catalyst was highly selective towards diester and diester products were obtained with excellent yields (80–100%).

Conclusion

In conclusion, we have developed a new magnetic nanosilica supported diacidic ionic liquid catalyst. The catalyst showed extraordinary catalytic activity in the esterification reaction of anhydrides and succinic acid with different alcohols to give corresponding diesters under solvent-free conditions. It is believed that the high-acidity of the ionic liquid together with Lewis acidity of Fe$_3$O$_4$ and high surface area of nanoparticles, might increase the activity of the synthesized catalyst. Furthermore, high-hydrophilicity of the catalyst as well as more hydrophilicity of monoester than diester led to excellent selectivity towards diester. The present study offers some other advantages such as easy recovery of the catalyst

by applying an external magnet, excellent product yields, operational simplicity and short reaction times. Moreover, the catalyst could be reused for at least 8 runs without any significant loss of its activity.

References

1. G. Wypych, *Handbook of Plasticizers*, 3rd edn. (Chem Tec Publishing, Ontario, 2017), pp. 1–6
2. J.K. Sears, J.R. Darby, *The Technology of Plasticizers*, 2nd edn. (Wiley, New York, 2003), pp. 1–200
3. J.S. Vrentas, C.M. Vrentas, J. Polym. Sci. Part B: Polym. Phys. **41**, 501 (2003)
4. H.C. Erythropel, S. Shipley, A. Bormann, J.A. Nicell, M. Maric, R.L. Leask, Polym. **89**, 18 (2016)
5. G.d. Yadav, M.S.M. Mujeebur Rahuman, Clean Technol. Environ. Policy **5**, 128 (2003)
6. A. Elomri, S. Mitaku, S. Michel, J. Med. Chem. **39**, 4762 (1996)
7. M.A. Ogliaruso, J.F. Wolfe, *Synthesis of Carboxylic Acids, Esters and Their Derivatives*, 1st edn. (Wiley, New York, 1991), pp. 1–250
8. H. Li, S. Yu, F. Liu, C. Xie, L. Li, Catal. Commun. **8**, 1759 (2007)
9. F. Chen, C. Lu, J. Nie, Z. Chen, G. Yang, Chem. Res. Chin. Univ. **32**, 219 (2016)
10. D.A. Morgenstern, U.S. Patent 20170029355A1 (2017)
11. M. Yudao, Q.L. Wang, H. Yan, X. Ji, Q. Qiu, Appl. Catal. A Gen. **139**, 51 (1996)
12. F.T. Sejidov, Y. Mansoori, N. Goodarzi, J. Mol. Catal. A Chem. **240**, 186 (2005)
13. H.B. Xing, T. Wang, Z.H. Zhou, Y.Y. Dai, Ind. Eng. Chem. Res. **44**, 4147 (2005)
14. V.R. Choudhary, K. Mantri, S.K. Jana, Micropor. Mesopor. Mater. **47**, 179 (2001)
15. V.R. Choudhary, K. Mantri, S.K. Jana, Catal. Commun. **2**, 57 (2001)
16. M. Salavati-Niasari, T. Khosousi, S. Hydarzadeh, J. Mol. Catal. A Chem. **235**, 150 (2005)
17. A. Mobaraki, B. Movassagh, B. Karimi, Appl. Catal. A Gen. **472**, 123 (2014)
18. Y.H. Liu, J. Deng, J.W. Gao, Z.H. Zhang, Adv. Synth. Catal. **354**, 441 (2012)
19. A. Maleki, Z. Hajizadeh, R. Firouzi-Haji, Micropor. Mesopor. Mater. **259**, 46 (2018)
20. S. Shaabani, A. Tavousi Tabatabaei, A. Shaabani, Appl. Organometal. Chem. **31**, 3559 (2017)
21. M. Borjian Boroujeni, A. Hashemzadeh, M.T. Faroughi, A. Shaabani, M.Mohammadpour Amini, RSC Adv. **6**, 100195 (2016)
22. A. Maleki, T. Kari, M. Aghaei, J. Porous Mater. **24**, 1481 (2017)
23. B. Mohammadi, L. Salmani, Asian J. Green Chem. **3**, 51 (2018)
24. M. Gholinejad, M. Razeghi, C. Najera, RSC Adv. **5**, 49568 (2015)
25. M.R. Mehrasbi, J. Mohammadi, M. Peyda, M. Mohammadi, Renew. Energy **101**, 593 (2017)
26. M. Zahedifar, P. Mohammadi, H. Sheibani, Lett. Org. Chem. **14**, 315 (2017)
27. S. Wang, Z. Zhang, B. Liu, J. Li, Catal. Sci. Technol. **3**, 2104 (2013)
28. A. Shaabani, H. Nosrati, M. Seyyedhamzeh, Res. Chem. Intermed. **41**, 3719 (2015)
29. A. Shaabani, R. Afshari, J. Coll. Interface Sci. **510**, 384 (2018)
30. A. Maleki, M. Aghaei, N. Ghamari, Appl. Organometal. Chem. **30**, 939 (2016)
31. A. Maleki, P. Zand, Z. Mohseni, RSC Adv. **6**, 110928 (2016)
32. A. Maleki, M. Ghassemi, R. Firouzi-Haji, Pure Appl. Chem. **90**, 387 (2018)
33. R. Fareghi-Alamdari, R. Hatefipour, Thermochim. Acta **617**, 172 (2015)
34. R. Fareghi-Alamdari, F. Ghorbani Zamani, M. Shekarriz, J. Mol. Liq. **211**, 831 (2015)
35. R. Fareghi-Alamdari, F. Ghorbani-Zamani, N. Zekri, RSC Adv. **6**, 26386 (2016)
36. R. Fareghi-Alamdari, R. Hatefipour, M. Rakhshi, N. Zekri, RSC Adv. **6**, 78636 (2016)
37. Z. Duan, Y. Gu, Y. Deng, J. Mol. Catal. A Chem. **246**, 70 (2006)
38. A.R. Hajipour, L. Khazdooz, A.E. Ruoho, Catal. Commun. **9**, 89 (2008)
39. N. Gupta, G.L. Kad, J. Singh, Catal. Commun. **8**, 1323 (2007)
40. F. Dong, G. Kai, S. Qunrong, L. Zuliang, Catal. Commun. **8**, 1463 (2007)
41. R. Fareghi-Alamdari, M. Nadiri, H. Hazarkhani, J. Mol. Liq. **227**, 153 (2017)
42. A.F. Alves, S.G. Mendo, L.P. Ferreira, M.H. Mendonca, P. Ferreira, M. Godinho, M.M. Cruz, M.D. Carvalho, J. Nanopart. Res. **18**, 27 (2016)
43. M. Mirjalili, F. Zahed, A. Hassanabadi, E- J. Chem. **9**, 1042 (2012)
44. S. Rostamizadeh, M. Nojavan, R. Aryan, M. Azad, Catal. Lett. **144**, 1772 (2014)
45. S.H. Jo, M.H. Lee, K.H. Kim, P. Kumar, Environ. Res. **165**, 81 (2018)
46. H. Valizadeh, E. Khalili, J. Iran. Chem. Soc. **9**, 529 (2012)
47. Z. Yingwei, L. Zhen, X. Chungu, Chin. J. Catal. **32**, 440 (2011)
48. H. Zhu, F. Yang, J. Tang, M. He, Green Chem. **5**, 38 (2003)
49. M. Arabi, M. Mohammadpour Amini, M. Abedini, A. Nemati, M. Alizadeh, J. Mol. Catal. A Chem. **200**, 105 (2003)
50. R. Thakkar, U. Chudasama, Green Chem. Lett. Rev. **2**, 61 (2009)

Affiliations

Reza Fareghi-Alamdari[1] · Mehri Nadiri Niri[1] · Hassan Hazarkhani[2] · Negar Zekri[1]

✉ Reza Fareghi-Alamdari
reza_fareghi@yahoo.com

[1] Faculty of Chemistry and Chemical Engineering, Malek-Ashtar University of Technology, Tehran, Iran

[2] Center for Research and Science Education, Organization for Educational Research and Planning, Tehran, Iran